Fluid Transport and the Dimensions of Cells and Interspaces of Living *Necturus* Gallbladder

KENNETH R. SPRING and ARVID HOPE

From the Laboratory of Kidney and Electrolyte Metabolism, National Heart, Lung, and Blood Institute, National Institutes of Health, Bethesda, Maryland 20014. Dr. Hope's present address is Department of Physiology, University of Bergen, N-5000 Bergen, Norway.

ABSTRACT The volume of the cells and lateral intercellular spaces were measured in living *Necturus* gallbladder epithelium. Under control conditions, the volume of the lateral spaces was 9% of the cell volume. Replacement of mucosal NaCl by sucrose or tetramethylammonium chloride (TMACl) caused intercellular spaces to collapse. During mucosal NaCl replacement, cell volume decreased to 79% of its control value. When NaCl was reintroduced into the mucosal bath, the intercellular spaces reopened and the cells returned to control volume. The NaCl active transport rate, calculated from the rate of cell volume decrease, was 266 pM/cm^2 ·s, close to the observed rate of transepithelial salt transport. It was calculated from the decrease in cell volume that all of the intracellular NaCl was transported out of the cell during removal of mucosal NaCl. The flux of salt across the apical membrane, calculated from the rate of cell volume increase upon reintroducing mucosal NaCl, was 209 pM/cm^2 ·s, in good agreement with estimates by other methods. The electrical resistance of the tight junctions was estimated to be 83.9% of the total tissue resistance in control conditions, suggesting that the lateral intercellular spaces normally offer only a small resistance to electrolyte movement.

INTRODUCTION

The importance of the lateral intercellular spaces in fluid transport by epithelial tissues was first pointed out by Whitlock and Wheeler (1964). Tormey and Diamond (1967) further refined and developed the concept that the spaces play a major role in the transepithelial transport of salt and water. Virtually all evidence implicating the lateral intercellular spaces in fluid movement came from electron micrographs of rabbit gallbladder fixed in different functional states. Data on the size and shape of the spaces derived from electron micrographs were subject to question because of the possibility of dimensional changes during fixation and embedding (Frederiksen and Rostgaard, 1974). We recently developed a chamber and optical arrangement which permitted the visualization of lateral intercellular spaces in a living *Necturus* gallbladder epithelium (Spring and Hope, 1978). Although other authors have reported visualization of the *Necturus* gallbladder intercellular spaces, they were not able to make quantitative determinations of interspace geometry (Frömter, 1972;

Loeschke et al., 1975). Voûte and Ussing (1968, 1970) made measurements of both the volume of lateral intercellular spaces and the thickness of epithelial cell layers in living frog skin preparations during short-circuiting. They were able to detect cell volume changes accompanying the passage of electric current and interspace changes accompanying alterations in hydrostatic pressure.

Tormey and Diamond (1967) published electron micrographs of rabbit gallbladder epithelium in transporting and non-transporting states. Diamond (1962) had previously observed that replacement of mucosal bathing medium NaCl by choline chloride or sucrose eventually halted fluid transport by fish gallbladder. Measurements of the rate of fluid transport, extracellular space, and tissue weight enabled Diamond to determine that fluid was transported for several minutes after the mucosal perfusate was made sodium-free. Tormey and Diamond (1967) observed that rabbit gallbladder cells decreased in volume after the mucosal NaCl was substituted by choline or sucrose. They also noted that the lateral intercellular spaces remained open until fluid transport stopped completely, several minutes after the mucosal substitution. They reasoned that the fluid transported after mucosal substitution must be derived from intracellular stores of NaCl and water. Because NaCl was not available to the epithelial cells from the mucosal surface, transported salt came from the cellular pool and the cells shrank in proportion to the quantity of solute lost. Fluid transport stopped when the cells were depleted of NaCl, cessation of fluid transport being indicated by the collapse of the lateral spaces.

We reproduced the mucosal NaCl replacement experiments of Diamond and colleagues in a living preparation. We mounted *Necturus* gallbladder in a miniature Ussing chamber (Spring and Hope, 1978). We were able to make continuous, accurate records of epithelial cell and interspace size and shape as a function of time after substitution of the mucosal NaCl by sucrose or TMACl (tetramethylammonium chloride). The changes in cell volume enabled estimates of the intracellular NaCl pool, NaCl active transport rate, and apical membrane NaCl permeability.

Changes in lateral intercellular space dimensions accompanied the alterations in *Necturus* gallbladder cell volume, and there was a correlation between variations in interspace dimensions and transepithelial electrical resistance. Ever since the tight junctions were shown to be leaky to small solutes (Ussing and Windhager, 1964), estimates have been made of the relative solute resistance of the tight junction and lateral intercellular spaces. Such estimates of the restriction to electrolyte movement posed by the tight junction varied widely depending on the dimensions chosen for the lateral intercellular spaces as well as the junction. Inasmuch as our experiments produced dimensions of the intercellular spaces concurrently with resistance data, we estimated the restriction to solute movement due to the lateral intercellular spaces. Several assumptions, which remain to be verified, were required to estimate that the junctional resistance comprised approximately 84% of the shunt resistance. The contribution of the lateral spaces to the total shunt resistance appeared to be small in control conditions, indicating that the spaces do not pose a major barrier to the movement of small solutes.

MATERIALS AND METHODS

Adult *Necturus maculosus* were obtained from Mogul Ed (Oshkosh, Wis.) and stored in aquaria at 15°C. They were anaesthetized by immersion in 0.1% tricaine methane sulfonate (Finquel, Ayerst Laboratories, New York), and the gallbladder was removed and drained of bile. The gallbladder was mounted in a miniature Ussing chamber as previously described (Spring and Hope, 1978). This chamber provided continuous perfusion of both the mucosal and serosal solutions, current and voltage electrodes in each bath, control of transepithelial hydrostatic pressure, and optimal optical properties. The serosal bath was continuously perfused with NaCl Ringer of the following composition: 90 mM NaCl, 10 mM $NaHCO_3$, 2.5 mM KCl, 0.5 mM NaH_2PO_4, 1.8 mM $CaCl_2$, 1.0 mM $MgCl_2$, 2.2 mM glucose, polyvinylpyrrolidone (PVP) 20 g/liter, pH 7.6, osmolality 210, gassed with 99% O_2, 1% CO_2. The mucosal bath was perfused at high rates either with NaCl Ringer, sucrose Ringer in which all NaCl and $NaHCO_3$ were substituted in equiosmolar amounts by sucrose, or tetramethylammonium chloride Ringer in which all NaCl and $NaHCO_3$ were replaced by TMACl. Sucrose and TMACl Ringer were bubbled with air and did not contain PVP or glucose. The mucosal flow rate was sufficiently great that a complete change in the composition of the mucosal fluid was achieved in 15–20 s ($t_1/_2$ = 4.5 s) enabling the measurement of biionic potentials as well as the time-course of tissue response.

The gallbladder chamber was placed on the stage of an inverted microscope (Diavert, E. Leitz, Inc., Rockleigh, N. J.) as shown in Fig. 1. The optical arrangement has been described previously (Spring and Hope, 1978). The preparation was illuminated with monochromatic light (495 nm) through a condenser-objective lens which formed a highly reduced image of the field stop diaphragm in the image plane. The microscope objective was an oil immersion lens (100 × 1.3 numerical aperture). This combination of lenses produced a contrasty image at × 1000 with a calculated lateral resolution of 0.3 μm and a calculated depth of field of 0.4 μm at 495 nm. Both lateral resolution and depth of field were evaluated experimentally and agreed with the calculated limits. Focusing through the preparation produced ~ 1-μm-thick optical sections of the tissue at the focal plane. We have shown previously (Spring and Hope, 1978) that there is a linear relationship between the cross-sectional area of a lateral intercellular space in the focal plane and the intensity of the light measured with a phototube placed over the image of the space. The microscope image was split in the housing of a photometer attachment and 90% of the light was diverted to a photomultiplier tube through an adjustable rectangular slit. This arrangement enabled the measurement of the light intensity profile of an interspace when the measuring slit was positioned over it and the microscope was focused from tight junction to basement membrane. The remaining 10% of the light from the microscope image was directed to an image intensified television camera (SIT 4410, Cohu Inc., Electronics Div., San Diego, Calif.). The output of the television camera was displayed on a monitor and stored on a video disk recorder (VDR-1R Arvin Echo, Echo Science Corp., Mountain View, Calif.). Time was displayed on the video disk records by a time code generator (9100–526, Datum Inc., Anaheim, Calif.), and the output of the disk was viewed on a second monitor. The television camera output was also connected to a video window generator (VWG-1, Telefactor Corp., Conshohocken, Pa.) and displayed on a third monitor. The window generator was used to monitor the position of the photometer measuring slit during measurements. During photometry with a conventional microscope it was not possible to see the location of the measuring slit in the microscopic field. This made it extremely difficult to accurately position the slit in a living preparation because small movements and focal changes occurred frequently. The window generator eliminated this limitation. The photometer measuring slit was back-

illuminated and projected onto the field of view during the set-up period prior to measurements. The back-illuminated slit appeared as a bright box in the television image, and the window generator was used to create a video window of the exact same size as the measuring slit. Thus, during measurements, the video image consisted of the epithelial cells with a superimposed slit produced by the window generator in the same position as the photometer slit.

The fine-focusing knob of the microscope was connected to a 10-turn potentiometer

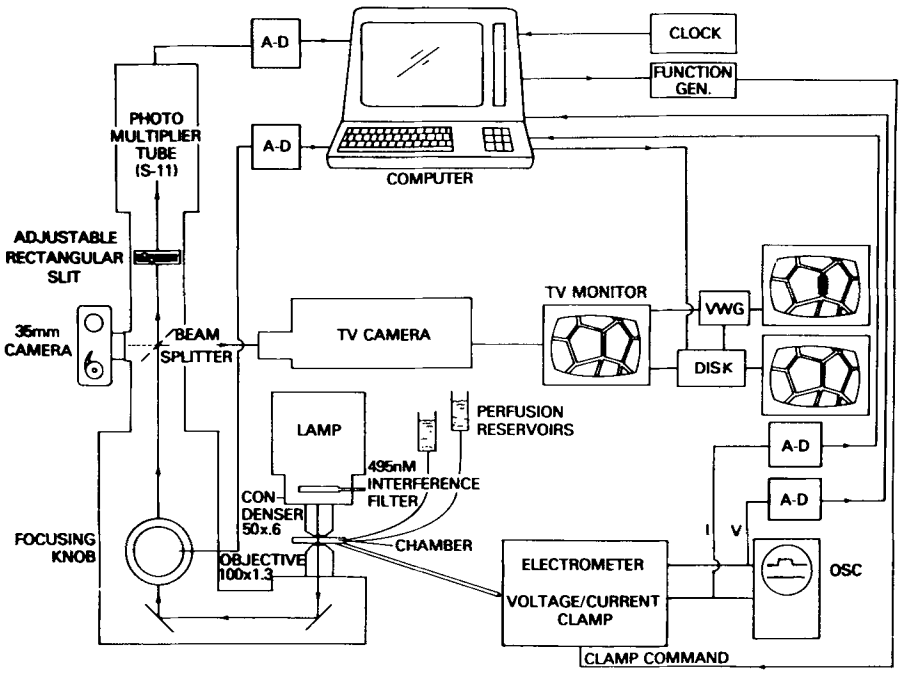

FIGURE 1. Block diagram of the experimental arrangement for visualization and measurement of epithelial cells and lateral intercellular spaces. The gallbladder chamber is shown diagrammatically on the stage of an inverted microscope. The image is divided at the beam splitter—90% of the light falls on the photomultiplier tube; 10% is diverted to the television camera. Microscope fine focus and photomultiplier current are digitized and sampled by the computer. The computer receives a time code signal from a clock and outputs voltage clamp commands via a function generator. Electrodes from the chamber permit voltage and current measurements which are also digitized and sampled by the computer. The video image is displayed on a monitor, stored on a video disk recorder, and mixed with the output of a video window generator (VWG).

powered by a 15-V supply; focus was thus read out electronically and compared with phototube current. Both of these signals were digitized by a multimeter (8500A, John Fluke Mfg. Co., Inc., Mountlake Terrace, Wash.) after being switched by a relay scanner (3495, Hewlett-Packard Co., Palo Alto, Calif.). The multimeter and scanner were controlled by a computer via the general purpose interface bus. The computer (4501, Tektronix, Inc., Beaverton, Ore.) received a time signal from the time code generator via an instrument coupler (4880, Fairchild Camera & Instrument Corp., San Jose, Calif.).

The computer also controlled the video disk operation. Transepithelial PD and resistance were measured by means of a combination electrometer-voltage clamp (Spring and Hope, 1978). Resistance was calculated from current and voltage changes during triangle wave (1 Hz) or square wave (100 ms) clamp commands.

Experiments were performed as follows: (*a*) an interspace and cell were chosen for study and the measuring slit was positioned;[1] (*b*) the microscope was focused at the level of the tight junction (the junctions were visible as a dark line at the cell boundaries); (*c*) the computer was ordered to begin sampling focal position, phototube current, and time; (*d*) every time the focus changed by 4 μm the computer ordered a video record of the field on video disc, along with records of phototube current, focus, and time; (*e*) when the basement membrane and underlying connective tissue were visualized the sampling sequence was ended. This sequence was rapidly performed (10–15 s) and anywhere from 6 to 13 video images of each cell recorded. The video disk records were used to determine cell size and shape. Each video frame contained one optical section of a cell at a known distance from the mucosal surface. The cell outline was traced and the coordinates of the tracing recorded by the computer. The cross-sectional area and perimeter of each tracing were then computed. All of the tracings from a single cell were then displayed in register in an orthographic projection of the cell. Cell volume and lateral surface area were computed from the thickness, area, and perimeter of each optical section of the cell.

All statistical and mathematical computations were carried out on the computer in either the on-line or off-line mode with programs written by the investigators in Basic. Values are expressed as the mean ± the standard error of the mean (SE).

TABLE I

CONTROL CELL DIMENSIONS

Cell height, μm	34.6±1.4*
volume, μm^3	22,500±1,200
mucosal area, μm^2	634±32
lateral area, μm^2	3,540±150

* Mean ± SE; n=32 cells.

RESULTS

Dimensions of the Average Cell and Interspace

The cross-sectional areas and heights of 32 gallbladder cells were determined when both perfusion solutions were NaCl Ringer. Table I lists the average dimensions of these cells. Cell height, determined as the distance from the level of the tight junctions to the level at which the underlying connective tissue appears, averaged 34.6±1.4 μm (SE). This is significantly greater than the height of 16.0±0.5 μm reported previously (Spring and Hope, 1978). In the previous study the tissue was tightly stretched to avoid movement during changes in hydrostatic pressure. Inasmuch as no hydrostatic pressure differences existed in the present study, the tissue was only lightly stretched to flatten folds in the epithelium. The cross-sectional area of the mucosal surface of the

[1] An interspace was acceptable for measurement if it was vertically oriented relative to the microscope optical axis and if the cell boundaries were sharply defined. A cell adjacent to the space was selected if the cell borders were clearly recognizable.

cells averaged 634±32 μm^2. Mean cell volume was 22,500±1,200 μm^3, and lateral surface area 3,540±150 μm^2. It should be noted that infoldings of the lateral cell membranes could not be accurately traced and were not included in the surface area computation. Similarly, because mucosal surface folds and microvilli could not be resolved, they were not traced in the area estimates.

Interspace volume in control conditions averaged 2,080 μm^3 per cell or ~ 9% of the mean control cell volume. The average interspace occupied a volume of 41 μm^3 per micrometer length of circumferential cell border. The average cell perimeter was 102 μm, the product of cell perimeter and interspace volume per micrometer of perimeter gave the volume of the space shared by two cells (4,196 μm^3).

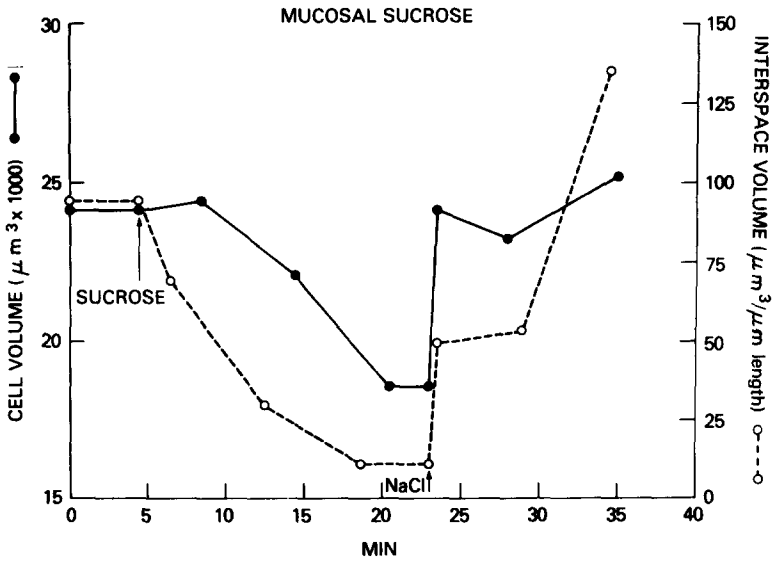

FIGURE 2. Records of cell volume and intercellular space volume in a typical NaCl-sucrose replacement experiment. At the first arrow mucosal NaCl was substituted by sucrose; at the second arrow sucrose was replaced by NaCl.

Replacement of Mucosal NaCl by Sucrose

When the mucosal perfusion solution was modified by replacement of all NaCl by sucrose, both cell and interspace volume decreased. The mucosal solution was rapidly switched from NaCl Ringer to sucrose Ringer. The solution change was typically complete in 20 s ($t_{1/2}$=4.5 s) as indicated by changes in the transepithelial potential difference and resistance. The time-course and magnitude of the typical changes in cell and interspace volume are shown for one experiment in Fig. 2. The control cell volume (●—●) was 24,113 μm^3; at the time indicated by the vertical arrow the mucosal solution was switched to sucrose Ringer. Over the next 15 min cell volume decreased to 18,512 μm^3, ~ 77% of the control value. At the same time, the volume of the lateral intercellular space adjacent to the cell decreased from the control volume of 94 $\mu m^3/\mu m$ to 10.8

$\mu m^3/\mu m$. The interspace volume decrease occurred more rapidly than the cell volume change. When the mucosal perfusate was switched back to NaCl Ringer, a rapid increase occurred in both cell and interspace volume. Cell volume increased within 30 s to 24,150 μm^3, a value comparable to the control volume. Successive measurements over the next 12 min showed no further changes in cell volume of any consequence. Interspace volume increased from 10.8 to 49.8 $\mu m^3/\mu m$ in the first 30 s after NaCl returned to the mucosal bath. A slow rise in interspace volume continued over the next 10 min until a volume of 134.5 $\mu m^3/\mu m$ was achieved. The intercellular space in this experiment was somewhat increased in volume compared to the control value, and it is uncertain whether this difference was due to measurement errors or represented a real volume increase.

Changes in cell and interspace volume in 12 experiments during sucrose substitution of mucosal NaCl are shown in Fig. 3. Fig. 3 A shows the decrease in cell volume after introduction of sucrose Ringer into the mucosal bath and the recovery of volume after reintroducing mucosal NaCl Ringer. Cell volume, expressed relative to the control value, is shown on the ordinate. After replacement of mucosal NaCl by sucrose, cell volume fell to 0.765 ± 0.025 (SE, $n = 12$) of control volume. This decrease was significant at the $P < 0.0001$ level. The initial rate of decrease in cell volume was calculated for each experiment by a linear least squares fit of the first two to three points after the solution change. The average rate of decrease for all 12 experiments was 4.5 ± 1.8 (SE) % min^{-1}. When NaCl was returned to the mucosal bath, cell volume increased to 0.96 ± 0.065 (SE, $n = 9$) of control volume. This value was not significantly different from 1.0, indicating that the cells returned to the control condition. The rate of increase of cell volume was 3.3 ± 0.8% min^{-1} (SE, $n = 7$) for those experiments in which the cells swelled after the return of mucosal NaCl.

Fig. 3 B shows the interspace volume ($\mu m^3/\mu m$ length) in spaces adjacent to the cells shown in the upper panel. The average control interspace volume of 47.4 ± 6.4 $\mu m^3/\mu m$ (SE, $N = 10$) decreased to 7.4 ± 1.8 $\mu m^3/\mu m$ during mucosal sucrose perfusion. A linear least squares fit of the initial decrease in interspace volume relative to control volume was done for each experiment. The average rate of decrease of interspace volume relative to the control volume was 7.9 ± 1.7 (SE) % min^{-1}, which differs significantly from zero at the $P < 0.001$ level. The minimum space volume achieved was 15.7% of the control volume. When NaCl was reintroduced into the mucosal bath the spaces swelled at an average rate relative to the control volume of 6.6 ± 1.6 (SE) % min^{-1}. The final average volume reached was 52.8 ± 13.7 $\mu^3/\mu m$ (SE, $n = 10$), not significantly different from the control volume of 47.4 $\mu m^3/\mu m$.

Replacement of Mucosal NaCl by TMACl

When the NaCl in the mucosal perfusion solution was substituted by equimolar TMACl, interspace volume decreased in a manner similar to that seen during the sucrose experiments. However, the time-course of cell volume change was very variable and differed from the sucrose substitution results. Fig. 4 shows a representative record of cell volume and interspace volume as a function of time. Cell volume (●——●) first increased when mucosal NaCl was replaced by

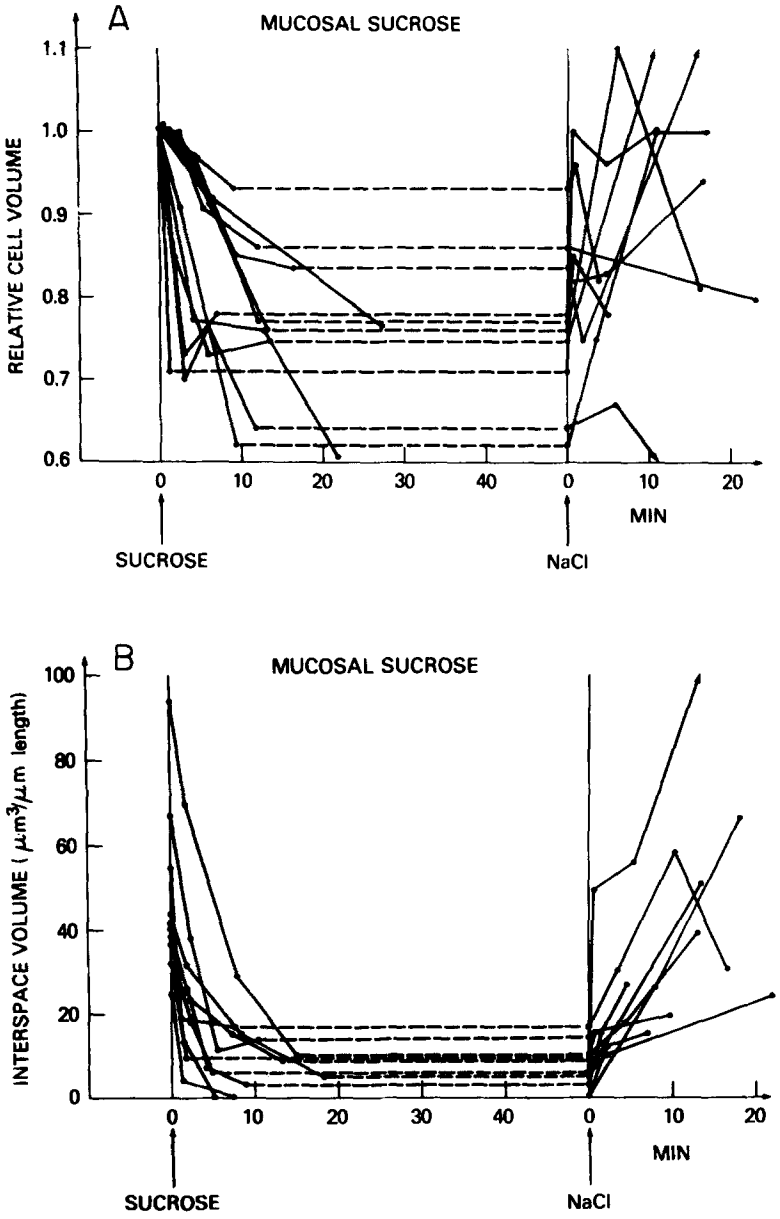

FIGURE 3. Records of 12 experiments in which mucosal NaCl was replaced by sucrose. (A) Cell volume relative to control as a function of time after replacement of mucosal NaCl by sucrose at time zero. At the second arrow, the mucosal perfusate was returned to NaCl Ringer. (B) Time-course of the volume of spaces adjacent to the cells in the top panel. Space volume is expressed as μm^3 per μm length of circumferential tight junction.

TMACl. The control cell volume of 17,997 μm^3 increased to 21,128 μm^3 5 min after the substitution. The cell then shrank to a volume of 15,990 μm^3 after a 25 min of mucosal perfusion, and finally slowly swelled to 18,715 μm^3. The final volume was virtually the same as the control volume and did not change very much when NaCl was reintroduced (volume after NaCl return was 18,245 μm^3).

Interspace volume (O- - -O) is given in Fig. 4. Control space volume was 74.1 $\mu m^3/\mu m$; it increased to 106.1 $\mu m^3/\mu m$ 2.5 min after TMACl perfusion began. The space then collapsed to a minimum volume of 26.6 $\mu m^3/\mu m$. 2 min after NaCl was reintroduced the space swelled to 44.1 $\mu m^3/\mu m$. Further measurements in this experiment were prevented because of technical difficulties.

Fig. 5 depicts the changes in cell and interspace volume in 12 TMACl substitution experiments. In Fig. 5 A cell volume, plotted relative to the control

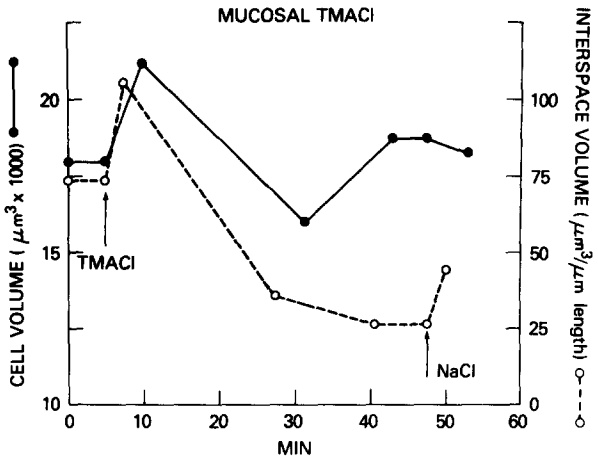

FIGURE 4. Records of cell volume and intercellular space volume in a NaCl-TMACl replacement experiment. At the first arrow mucosal NaCl was substituted by TMACl; at the second arrow TMACl was replaced by NaCl.

value, showed a variable time-course and pattern. In all experiments, however, there was a fall in cell volume at some time during the TMACl perfusion. This decrease in volume was sometimes followed by slow cell swelling. The average minimum cell volume was 0.821 ± 0.031 (SE, n = 12) relative to a control volume of 1.0. This value was significantly less than the control at the $P < 0.001$ level. The average slope of the decreasing phase of cell volume was 4.3 (±1.1):% min^{-1} (SE, n = 12) relative to the control volume. The rate of decrease in cell volume was not different from that seen in the sucrose experiments. When NaCl returned to the mucosal bath the cells swelled back to their original volume. Final volume was 1.09 ± 0.08 (SE, n = 9) times the control value, not significantly different from 1.0. When NaCl replaced mucosal TMACl, only four cells showed a monotonic increase in volume. The initial slope of the cell volume increase of these cells was pooled with the observations after cessation of sucrose perfusion. The average slope obtained was 4.5 (±0.8)% min^{-1} (SE, n =

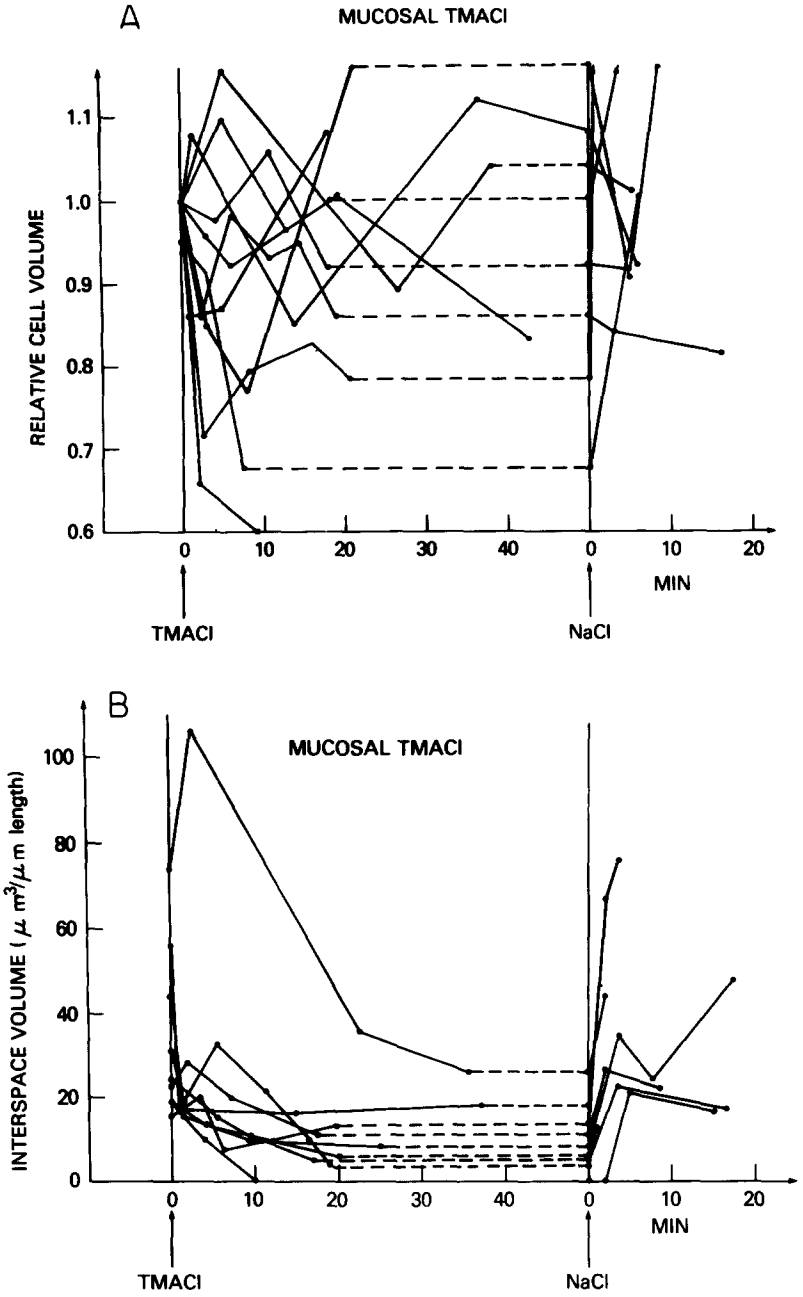

FIGURE 5. Records of 12 experiments in which mucosal NaCl was replaced by TMACl. (A) Cell volume relative to control as a function of time after replacement of mucosal NaCl by TMACl at time zero. At the second arrow, the mucosal perfusate was returned to NaCl Ringer. (B) Time-course of the volume of spaces adjacent to the cells in the top panel. Space volume is expressed as μm^3 per μm length of circumferential tight junction.

11). All of the parameters for cell volume changes during sucrose or TMACl perfusion are summarized in Table II.

Fig. 5 B depicts the time-course of interspace volume in nine spaces adjacent to the cells in the upper panel. Interspace volume averaged 34.1 ± 6.6 $\mu m^3/\mu m$ (SE, n = 9) during NaCl perfusion before TMACl substitution. After TMACl substitution interspace volume fell to 10.1 ± 2.5 $\mu m^3/\mu m$, a significant change at the $P < 0.01$ level. The linear least squares fit of individual experiments gave an initial rate of decrease of interspace volume relative to the respective control volumes of 5.0(±1.2)% min^{-1}. This rate of decrease of interspace volume in the TMACl experiments was not significantly different from that in the sucrose substitution experiments. The pooled rate of interspace decrease was 6.6(±1.1)% (n = 18) for both experimental conditions. Minimum interspace volume during mucosal TMACl perfusion was 29.5% of the control value. When the NaCl returned to the mucosal bath, the space volume increased to a mean value of 27.9 ± 5.8 $\mu m^3/\mu m$ (SE, n = 7), not significantly different from

TABLE II

RELATIVE CELL VOLUME CHANGES DURING MUCOSAL SUCROSE OR TMACl

Mucosal perfusate	Cell volume* $\frac{\text{experimental}}{\text{control}}$	n	Initial slope*	n
Sucrose Ringer	0.76±0.03	12	−0.045±0.018	12
NaCl	0.96±0.065	9	0.033±0.008	7
TMACl Ringer	0.82±0.03	12	−0.043±0.011	12
NaCl	1.09±0.08	9	0.066±0.009	4

Steady-state cell volume is expressed as a fraction of the control volume for conditions in which the mucosal perfusate NaCl was replaced by sucrose or TMACl. The initial slope refers to the initial rate of change of cell volume relative to the control volume after alteration of the mucosal perfusate.
* Mean ± SE.

the control value. The rate of space increase could not be accurately determined in these experiments because of considerable variability in the results. The changes in interspace volume during both TMACl and sucrose substitution are summarized in Table III.

Table III also shows that the mean control volumes of the interspaces in both groups of experiments were not significantly different. A pooled control space volume of 41.4 ± 4.7 $\mu m^3/\mu m$ (SE, n = 19) was calculated. The minimum interspace volume also did not differ between the two groups and a pooled minimum volume was computed as 8.7 ± 1.5 $\mu m^3/\mu m$. The interspace volume recovered to the control value in both groups after NaCl returned to the mucosal bath. The pooled space volume was 39.8 ± 7.5 $\mu m^3/\mu m$ (SE, n = 17), not significantly different from the control value before the substitution experiment.

Fig. 6 shows a composite picture of the average change in cell and interspace volume in a mucosal Na^+ or NaCl substitution experiment. The cell decreases in

volume from a control value of 1.0 to a minimum of 0.79 during the substitution and then returns to 1.03 of the control volume after NaCl is reintroduced. The rates of decrease and increase of cell volume relative to control volume shown are the mean values for the combined results of the sucrose and TMACl experiments. The rate of cell volume decrease is 4.4% min^{-1} and the rate of increase is 4.5% min^{-1}. Interspace volume decreases from the control value of 1.0 to a minimum of 0.21 during the substitution and then returns to 0.97 of the control volume after NaCl is reintroduced. The pooled rate of interspace volume decrease relative to control volume is 6.6% min^{-1}. The rate of space increase in Fig. 6, 6.6% min^{-1}, comes from the sucrose experiments only because of the variability in the TMACl experiments.

The decrease in cell volume which occurred when mucosal NaCl was removed represented a loss of solute from the cell. Since the osmolality of the perfusates

TABLE III

INTERSPACE VOLUME DURING MUCOSAL SUCROSE OR TMACl

Mucosal perfusate	n	Interspace volume*	P
		$\mu m^3/\mu m$	
NaCl Ringer	10	47.4±6.4	
Sucrose Ringer	10	7.4±1.8	<0.0001
NaCl Ringer (recovery)	10	52.8±13.7	NS
NaCl Ringer	9	34.1±6.6	
TMACl Ringer	9	10.1±2.5	<0.01
NaCl Ringer (recovery)	7	27.9±5.8	NS
Pooled NaCl Ringer	19	41.1±4.7	
Pooled Sucrose-TMACl	19	8.7±1.5	<0.0001
Pooled recovery	17	39.8±7.5	NS

Steady-state interspace volume during substitution of mucosal NaCl by sucrose or TMACl. Volume is given in μm^3 per μm of circumferential junctional length.
* Mean ± SE.

was always the same (214 mosmol), cell osmolality should not change during the removal of mucosal NaCl. The cell volume decrease was then directly related to a loss of intracellular solute. The observed 21% decrease in cell volume was equivalent to a loss of 45 mosmol of osmotically active solute. Intracellular NaCl in Necturus gallbladder has been estimated by van Os and Slegers (1975) to be about 30 mM/kg wet weight and intracellular Na activity is reported to be around 12–15 mM (Graf and Giebisch, 1977). If all intracellular NaCl were lost, during removal of mucosal NaCl cell volume would decrease by 18–27%. The cell volume changes in our experiments are in good agreement with this calculation.[2] Intracellular NaCl could exit from the cell by diffusing across the

[2] Further support for the conclusion that the cell volume decrease is associated with the loss of intracellular NaCl comes from our recent observations of ion activities in *Necturus* proximal tubule cells. Intracellular chloride activity decreased from 24mM to 11mM during removal of mucosal NaCl (Spring and Kimura, 1978). Intracellular Na^+ activity follows a similar pattern during removal of mucosal NaCl (Kimura and Spring, manuscript submitted for publication).

apical membrane, or it could be transported out of the cell by the pump in the basolateral membrane. The diffusional NaCl flux out of the cell during sucrose Ringer perfusion, was calculated from the electrochemical gradients and apical ion permeabilities (Reuss and Finn, 1975 *b*) and was found to constitute <20% of the total salt loss. A portion of the change in cell volume could also be due to intercellular fluid loss across the apical membrane because of a higher reflection coefficient for sucrose (or TMA) than for NaCl. Inasmuch as the apical membrane is relatively tight to solute (Reuss and Finn, 1975 *b*; van Os and Slegers, 1975) the reflection coefficients for sucrose, TMACl and NaCl are

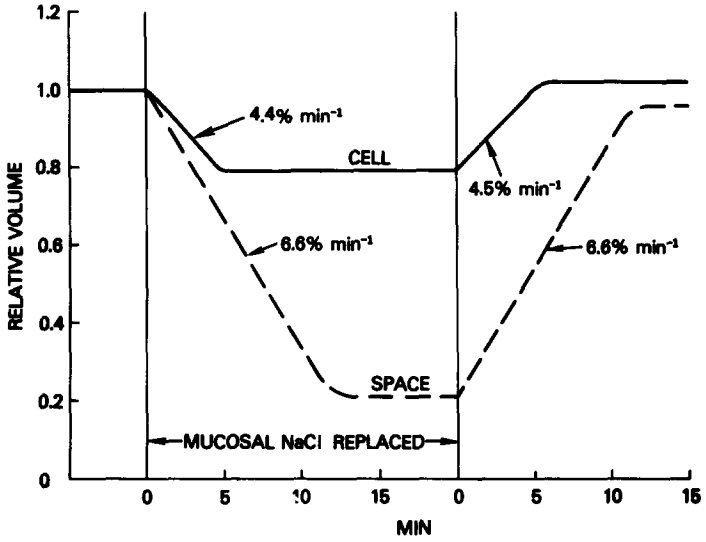

FIGURE 6. Composite picture of average changes in cell and intercellular space volume as a function of time during replacement of mucosal NaCl. The parameter values for each curve are given in the text.

probably all near one across this membrane and little change in volume flow would be expected. The most likely explanation for the cell volume shrinkage upon replacement of mucosal NaCl is that offered by Diamond (1962): the cell shrinkage is secondary to transport of the intracellular stores of NaCl. Accepting this explanation, the initial rate of cell volume decrease may be used to estimate the active transport rate. Because NaCl cannot enter the cell across the apical membrane when the mucosal bath is Na-free, the rate of decrease of cell volume (4.4% min^{-1}) is determined primarily by the rate of transport of NaCl across the basolateral border. From the control cell volume and the rate of decrease of cell volume we can calculate the isotonic NaCl flux out of the cell. The NaCl flux per cm^2 of mucosal surface area is 266 ± 87 (SE) × 10^{-12} $M/cm^2 \cdot s$ in reasonable agreement with the estimates of net NaCl transport from fluid absorption (306 × 10^{-12} $M/cm^2 \cdot s$, van Os and Slegers, 1975; 134 × 10^{-12} $M/cm^2 \cdot s$, Spring and Hope[3]).

[3] Spring, K. R., and A. Hope. Unpublished data.

The initial rate of cell swelling after the return of mucosal NaCl may be used to determine the NaCl influx into the gallbladder cell across the apical membrane. We assume that intracellular NaCl concentration was sufficiently low so that active transport may be neglected during the initial increase in cell volume. Cell volume increased at a rate of 4.5% per minute and the influx of NaCl may be calculated from the mucosal surface area, average minimum cell volume and a mucosal NaCl concentration of 100 mM. The flux thus obtained, 209 ± 47 (SE) $\times 10^{-12}$ M/cm^2·s, is not significantly different from the estimated active transport rate ($266 \pm 87 \times 10^{12}$ M/cm^2·s) and is in good agreement with current estimates of Na influx from electrophysiological (Reuss and Finn, 1975 *a*, *b*; van Os and Slegers, 1975) and tracer (Graf and Giebisch, 1977) experiments. Theoretical model calculations (Weinstein and Stephenson, 1978) also yield a comparable estimate of NaCl influx across the apical membrane. If the influx of NaCl were electrically neutral, the electrical gradient across the apical membrane could be disregarded and an apical membrane NaCl permeability may be calculated as 2.1×10^{-6}cm/s. This value agrees well with current estimates of apical permeability in Necturus gallbladder (van Os and Slegers, 1975; Reuss and Finn, 1975 *b*; Weinstein and Stephenson, 1978) and in Necturus proximal tubule cell (Spring and Giebisch, 1977).

Transepithelial Resistance and Interspace Dimensions

Measurements of the cross-sectional area and depth of the lateral intercellular spaces may be used to estimate the electrical resistance of the spaces. If the conductivity of the solution within the interspaces is near that of Ringer's solution, it is possible to calculate the fraction of tissue electrical resistance attributable to the spaces. Epithelial electrical resistance is typically calculated in ohms · cm^2, assuming a smooth mucosal surface. For the purpose of calculation, it was necessary to determine the length of intercellular junction per cm^2 of mucosal surface. This was estimated, using enlarged photographs of the mucosal surface of gallbladders. We measured the length of the tight junction surrounding gallbladder cells, and the circumferential length of junction averaged 862 cm/cm^2 of epithelium. In control conditions, the lateral spaces were very narrow (<0.3 μm) in a region 4–6 μm beneath the tight junction. Since the width of this region could not be accurately estimated optically, the space resistance was calculated only for the clearly visible portion of the interspace (width >0.3 μm). The interspace resistance determined for the visible portion averaged 4.9 ± 0.6 ohm · cm^2, while transepithelial resistance was 280 ± 21 ohm · cm^2 ($n = 15$) in NaCl Ringer solution. Transepithelial resistance is made up of the resistance of two parallel pathways—the cells and the intercellular shunts. Inasmuch as the cellular path resistance is at least ten times the shunt resistance (Frömter, 1972; Reuss and Finn, 1975 *a*), we ignore it in the following calculations. Transepithelial resistance, R, is then approximately given by:

$$R \simeq R_{TJ} + R^{I}_{Lis} + R^{V}_{Lis}, \quad (1)$$

where R_{TJ} is the junctional resistance, R^{I}_{Lis} the resistance of the lateral spaces which are not clearly visible, R^{V}_{Lis} the resistance of the clearly visible spaces.

In experiments in which lateral space dimensions change, it may be possible to estimate the resistive contribution of both the junction and invisible portions of the interspace. If the poorly visible portion of the interspace does not differ in its mechanical properties from the wider, visible region, it is reasonable to assume that the invisible portion of the interspace changes its width in proportion to changes in the visible space. Eq. 1 may then be rewritten as:

$$R \simeq R_{TJ} + R^{V}_{Lis}(\alpha + 1), \tag{2}$$

where α is some proportionality factor relating the change in the narrow, invisible region of the interspace to the wider, more clearly visible region. A plot of total tissue resistance, R, against the resistance of the lateral spaces which are clearly visible should have as its intercept R_{TJ}, the junctional resistance, and as its slope $(\alpha + 1)$, the proportionality factor. We analyzed, by Eq. 2, all of the experiments in which lateral space varied. In all cases we used measurements of space dimensions when the mucosal bath contained NaCl Ringer to avoid changes in junctional resistance due to alterations in mucosal bath composition. For example, tissue resistance and space dimensions were compared after mucosal sucrose had been replaced by NaCl Ringer. During the ~ 5 min it took the spaces to reopen to normal size, it was possible to make two to four simultaneous determinations of resistance and interspace dimensions. Resistance and interspace dimension measurements were made in a number of different experimental conditions: (*a*) with NaCl in the mucosal bath after mucosal sucrose or TMACl Ringer perfusion (n = 9); (*b*) during perfusion of ouabain (1 mM) in the serosal bath (n = 4); (*c*) during the passage of transepithelial constant current (n = 2). Ouabain in the serosal bath led to eventual collapse of the spaces and an increase in tissue resistance. Transepithelial current flow also altered space dimensions. Mucosa positive current caused the spaces to enlarge, whereas mucosa negative current resulted in a narrowing of the spaces. Fig. 7 shows some representative plots of tissue resistance (ordinate) against calculated interspace resistance on the abscissa. If the preceding assumptions and analysis are correct, the intercepts of the plots correspond to the junctional resistance because interspace resistance is zero. The slopes of the fitted lines represent the proportionality factor $(\alpha + 1)$ and give an indication of the resistance due to the narrow, invisible region of the space. The slope was consistently around 10, indicating that the major portion of the resistance change of the interspace lay in the poorly visible region near the junction. By pooling all of the fitted lines and adjusting them relative to their control resistance values, the junctional resistance was estimated to be 235 ± 20 Ω cm^2, or 83.9 ± 3.2% (n = 15) of the control tissue resistance. This value is significantly < 100% at the $p < 0.0001$ level. The visible portion of the spaces represented only ~ 2% of the shunt resistance, and the poorly visible interspaces ~ 14% of the shunt resistance. Therefore, visualization of the spaces was only of limited help in obtaining estimates of junctional resistance because of relative importance of regions of interspace too narrow to be accurately measured.

DISCUSSION

Necturus gallbladder epithelial cells are large and regularly shaped. The relatively simple geometry of this epithelium has enabled us to clearly visualize the

lateral spaces and to delineate cell outlines. However, our estimates of cell and interspace volume are considerably more accurate than the values for mucosal and lateral cell membrane surface areas. As mentioned in Results, we did not attempt to trace the small folds and irregularities of the lateral cell borders. Resolution of such small details with the bright-field optics employed was not possible. It is likely that more accurate estimates of mucosal and lateral cell membrane areas in living preparations could be made with differential interference contrast optics such as those employed by Dibona (1978) in his elegant observations of the surface of the toad urinary bladder. Blom and Helander (1977) showed that the mucosal surface area of fixed rabbit gallbladder epithelial

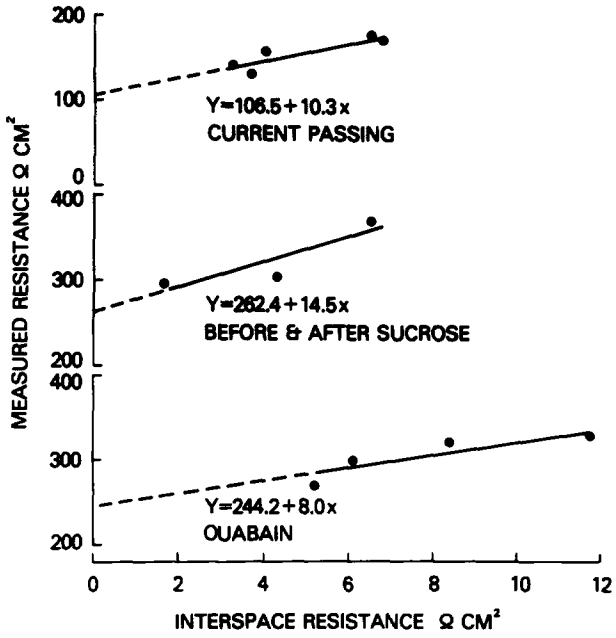

FIGURE 7. Measured tissue electrical resistance, on the ordinate, is plotted as a function of the calculated resistance of the visible portion of the lateral intercellular space. Examples of the relationship are shown for three groups: current passage (top), before and after a period of substitution of mucosal NaCl by sucrose (middle), and during the application of 1 mM serosal ouabain (bottom).

cells was increased 4.6–6.4 times over the smooth surface area because of microvilli. They also reported that lateral surface membranes were similarly increased, compared to the smooth surface area, from 3- to 4.4-fold by ridges and projections. The extent of increase in mucosal and lateral surface areas relative to the smooth surface areas reported here of *Necturus* gallbladder cells is unknown at present. The volume of the lateral intercellular spaces of *Necturus* gallbladder is 9% of cell volume. Blom and Helander (1977) measured interspace volumes of 11–28% of cell volume in fixed rabbit gallbladder. The large cells and intercellular spaces of *Necturus* gallbladder make it more suitable for detailed optical investigations than the rabbit gallbladder.

Direct microscopic observation of the cells and intercellular spaces of living *Necturus* gallbladder epithelium demonstrated that the lateral intercellular spaces collapsed under conditions in which fluid transport was abolished. We had previously observed that intercellular spaces were extremely narrow or not visible during perfusion with sulfate Ringer (Spring and Hope, 1978), a condition which stops fluid transport. Replacement of mucosal NaCl by TMACl or sucrose also resulted in collapse of the lateral spaces. Although fluid transport was not measured in these experiments, on the basis of previous results (Diamond, 1962) it could be expected to cease after removal of mucosal NaCl. Shrinkage of the epithelial cells upon removal of mucosal NaCl is also consistent with previous observations in both rabbit gallbladder (Tormey and Diamond, 1967) and fish gallbladder (Diamond, 1962). We have shown previously that the lateral spaces in *Necturus* gallbladder were maintained open by an extremely small difference in hydrostatic pressure of ~ 3-cm H_2O (Spring and Hope, 1978). Collapse of the spaces is presumably secondary to a decrease in the hydrostatic pressure within the spaces. The pressure in the spaces is thought to result from fluid flow driven by active solute transport (Diamond and Bossert, 1967). Support for this sequence of events came from electron micrographs of rabbit gallbladder fixed in different functional states (Kaye et al., 1966; Tormey and Diamond, 1967; Blom and Helander, 1977).

The composite picture of the cell volume transients (Fig. 6) was utilized to calculate the flux of NaCl into and out of the epithelial cells. Removal of mucosal NaCl resulted in a decrease of both cell and interspace volume. The decrease in cell volume must have been secondary to the loss of solute from the cells. The amount of solute lost agreed well with estimates of total cell NaCl, and we concluded that virtually all of the intracellular NaCl is directly or indirectly available to be transported. These results do not permit us to determine whether all intracellular NaCl is immediately accessible to the transport pool or is available only after emptying of other cellular Na compartments into the transport pool. The rate of cell volume decrease was reasonably close to the normal rate of transepithelial NaCl and water transport. The rate of collapse of the lateral intercellular spaces relative to their control volume was greater than the rate at which the cells decreased in volume compared to their control volume. Inasmuch as the absolute volume of the average interspace is about 9% of cell volume, the decrease in cell volume observed (21%) is nearly 2.5 times greater than the decrease in interspace volume. The rate of active transport by the cells would be expected to decrease as the cell sodium falls, and the interspaces would be predicted to collapse as transport slowed. Inasmuch as the kinetic relationship between transport and intracellular concentration is unknown in *Necturus* gallbladder, it is not possible to determine the quantitative influence of changes in transport rate on interspace volume. In addition, if the tight junctions allow a significant flux of water across them, fluid from the spaces could move directly into the mucosal bath because of differences in solute reflection coefficients. It is probable that the relatively large molecular size of sucrose or TMACl results in higher reflection coefficients for them across the tight junction than for NaCl. Replacement of mucosal NaCl by isoosmotic sucrose or TMACl would lead to differences in effective osmolality across the

junction and subsequent transjunctional water flow. Such a phenomenon could accelerate the collapse of the intercellular spaces compared to what would occur solely as the result of decreased cellular active transport. When NaCl is reintroduced into the mucosal bath, the lateral intercellular spaces reopen at a rate similar to that seen during space collapse. The time-courses of space opening and collapse were identical in spite of differences in the route of fluid movement. When the spaces open, the fluid presumably comes from the cells and moves in response to solute transport. The reflection coefficient effects discussed above are probably absent under these circumstances since NaCl is present in both baths at the same concentration.

Our observations of the magnitude and rates of cell volume change during removal of mucosal NaCl strongly support the conclusions of Diamond and colleagues. The dynamic behavior of the spaces in the living preparation agree well with the results from electron micrographs of fixed tissue. Necturus gallbladder cells change volume in response to removal of mucosal NaCl in a manner completely consistent with the earlier observations of Diamond in fish gallbladder and Tormey and Diamond in rabbit gallbladder. In addition, the electrical data indicate that the primary barrier to extracellular ion flow lies at the level of the tight junction in *Necturus* gallbladder.

Received for publication 10 July 1978.

REFERENCES

BLOM, H., and H. F. HELANDER. 1977. Quantitative electron microscopical studies on in vitro incubated rabbit gallbladder epithelium. *J. Membr. Biol.* **37**:45–61.

DIAMOND, J. M. 1962. The reabsorptive function of the gallbladder. *J. Physiol. (Lond.).* **161**:442–473.

DIAMOND, J. M., and W. H. BOSSERT. 1967. Standing-gradient osmotic flow. *J. Gen. Physiol.* **50**:2061–2083.

DIBONA, D. R. 1978. Direct visualization of epithelial morphology in the living amphibian urinary bladder. *J. Membr. Biol.* In press.

FREDERIKSEN, O., and J. ROSTGAARD. 1974. Absence of dilated lateral intercellular spaces in fluid-transporting frog gallbladder epithelium. *J. Cell Biol.* **61**:830–834.

FRÖMTER, E. 1972. The route of passive ion movement through the epithelium of *Necturus* gallbladder. *J. Membr. Biol.* **8**:259–301.

GRAF, J., and G. GIEBISCH. 1977. Intracellular sodium activity and sodium transport in *Necturus* gallbladder epithelium. *Proc. Int. Union Physiol. Sci. (Paris).* **13**:277.

KAYE, G. I., H. O. Wheeler, R. T. WHITLOCK, and N. LANE. 1966. Fluid transport in the rabbit gallbladder. *J. Cell Biol.* **30**:237–268.

LOESCHKE, K., G. M. EISENBACH, and C. J. BENTZEL. 1975. Water flow across *Necturus* gallbladder and small intestine. *Excepta Med. Int. Cong. Ser.* **391**:406–411.

REUSS, L., and A. L. FINN. 1975 *a*. Electrical properties of the cellular transepithelial pathway in *Necturus* gallbladder. I. Circuit analysis and steady-state effects of mucosal solution ionic substitutions. *J. Membr. Biol.* **25**:115–139.

REUSS, L., and A. L. FINN. 1975 *b*. Electrical properties of the cellular transepithelial pathway in *Necturus* gallbladder. II. Ionic permeability of the apical cell membranes. *J. Membr. Biol.* **25**:141–161.

SPRING, K. R., and G. GIEBISCH. 1977. Kinetics of Na^+ transport in *Necturus* proximal tubule. *J. Gen. Physiol.* **70**:307–328.

SPRING, K. R., and A. HOPE. 1978. Size and shape of the lateral intercellular spaces in a living epithelium. *Science (Wash. D.C.).* **200**:54–58.

SPRING, K. R., and G. KIMURA. 1978. Chloride reabsorption by renal proximal tubules of *Necturus*. *J. Membr. Biol.* **38**:233–254.

TORMEY, J. M. and J. M. DIAMOND. 1967. The ultrastructural route of fluid transport in rabbit gallbladder. *J. Gen. Physiol.* **50**:2031–2060.

USSING, H. H., and E. E. WINDHAGER. 1964. Nature of shunt path and active sodium transport path through frog skin epithelium. *Acta Physiol. Scand.* **61**:484–504.

VAN OS, C. H., and J. F. G. SLEGERS. 1975. The electrical potential profile of gallbladder epithelium. *J. Membr. Biol.* **24**:341–363.

VOÛTE, C. L., and H. H. USSING. 1970. Quantitative relation between hydrostatic pressure gradient, extracellular-volume and active sodium transport in the epithelium of the frog skin *(R. Temporaria). Exp. Cell. Res.* **62**:375–383.

VOÛTE, C. L., and H. H. USSING. 1968. Some morphological aspects of active sodium transport. *J. Cell Biol.* **36**:625–638.

WEINSTEIN, A. M., and J. L. STEPHENSON. 1978. Transport across a simple epithelium. *Fed. Proc.* **37**:569.

WHITLOCK, R. T., and H. O. WHEELER. 1964. Coupled transport of solute and water across rabbit gallbladder epithelium. *J. Clin. Invest.* **43**:2249–2265.